Features of radiation damage of Ni-Ti alloy under exposure to heavy ions of gaseous elements

V P Poltavtseva[1], S B Kislitsin[1], D A Satpayev[1], T S Mylnikova[2] and A V Chernyavskii[2]

[1] Institute of Nuclear Physics, Almaty, Republic of Kazakhstan

[2] National Research Tomsk Polytechnic University, Tomsk, Russia

E-mail: poltavtseva@inp.kz

Abstract. The consistent patterns of changes in structural and phase state, hardening and temperature ranges of martensitic transformations in Ni-Ti alloy with the shape memory effect after implantation of heavy ions $_{16}O^{3+}$, $_{40}Ar^{8+}$ and $_{84}Kr^{15+}$ under comparable parameters have been experimentally studied. It is found that under the impact of $_{84}Kr^{15+}$ ions, a two-layer surface structure with radiation-hardened second layer is formed, radiation-stimulated phase transformation B19'→B2 occurs in the near-surface layer and out-range area, and the martensitic transformation temperature increases toward higher values after implantation of $_{40}Ar^{8+}$ and $_{84}Kr^{15+}$ ions.

1. Introduction

Modification of materials by heavy ion implantation has become a promising technology. It is important to know which heavy ions are most effective in terms of creating radiation-resistant titanium nickelide alloys to be applied in nuclear power engineering or coatings for medical supplies.

Previously it was found [1–3] that modification by heavy krypton ions of low and high energy in the two-phase Ni-Ti alloy with the shape memory effect does not cause amorphization of Ti-Ni phases. Radiation-stimulated phase transformation B19'→B2 occurs, which is the major cause of deterioration of its physical-mechanical and functional properties, and temperatures ranges of martensitic transformation extend. In the case of implantation of high-energy krypton ions, a globular structure is formed on the Ni-Ti alloy surface and the degree of its homogeneity decreases as the fluence increases, radiation hardening is found to occur in the out-range area at low (~ 10^{13} ion/m^2) fluences due to the reduced size of the structural fragments of Ni-Ti phases.

In [4,5], it is also shown that consistent high-energy krypton ion implantation and application of high-current electron beam increases the quality of the Ni-Ti alloy surface. In the out-range area, it causes formation of primary martensite phase B19' responsible for the shape memory effect, formation of nano-sized particles of NiTi R-phase, increase in the temperature interval of the martensitic transformation and further softening. In [6,7], it is found that the distinguishing feature of a purely thermal effect on the structure of Ni-Ti alloy formed by ion implantation is hardening caused by the ordering of the radiation defect structures (phases).

The paper presents the experimental results to show the effect of implantation of different heavy ions of gaseous elements on the structural and phase state, and physical and mechanical properties of Ni-Ti alloy with the shape memory effect.

2. Experimental methods and material

We studied Ni-Ti alloy with Ni of 53.46 wt.% and Ti of 46.54 wt.%, preferably consisting of NiTi with the B2 structure (austenite), NiTi with B19 structure (martensite) and a minor content of Ti, excess Ni in the form of solid solution and process particles similar in composition to $Ti_2Ni(C)$ [8]. Before implantation, a proven technology was used to prepare the surface of the samples: cutting out by spark cutting across the massive forged plate of semiindustrial Ni-Ti alloy, mechanical polishing with skins of different grits and buffing with GOI paste. The sample size was $15.000\times\sim3900\times3500$ μm^3.

The data of preliminary testing were used to choose Ni-Ti alloy with the titanium nikelid phase ratio B19'/B2 equal to ~ 0.7 which showed the highest values of martensitic transformation characteristic temperatures compared to those for higher values of the phase ratio.

Implantation of $_{16}O^{3+}$, $_{40}Ar^{8+}$ and $_{84}Kr^{15+}$ ions under relatively equal parameters A/Z = ~ 5.3; energies E_{ion}=1.75 MeV/a.e.m. (28.70 and 147 MeV, respectively), fluence $\Phi=10^{19}$ ions/m^2 and beam current J_{beam}=1.0–0.85 μA was performed with DC-60 cyclotron (Astana, Kazakhstan). The damaged area was ~ 1×10^{-4} m^2.

Testing of the samples before and after implantation was performed by X-ray diffraction analysis, scanning electron microscopy, measuring microhardness and the shape memory effect with D8 ADVANCE diffractometer, JSM-7500F (JEOL) microscope, microhardness tester PMT-3M and an apparatus for measuring the temperature hysteresis of the electrical resistance.

3. Experimental results and discussion

SEM studies at low magnifications revealed that in the case of $_{16}O^{3+}$ion implantation, traces of sputtering, i.e. tuberosity, pits, remnants of $Ti_2Ni(C)$ process particles are observed on the Ni-Ti alloy surface. As the ion mass increases 2.5 times as much (ions $_{40}Ar^{8+}$), the surface becomes smoother with little roughness. Part of the particles protrudes over the surface which indicates that ion etching occurs alongside with sputtering. In case of heavier $_{84}Kr^{15+}$ ions, etching completely dominates.

Higher magnification of SEM-images indicates formation of bright particles of a round shape, bubbles of about 1 nm, and tracks of 8 to 25 nm or conglomerates made up of several tracks with a dome, and circular bubble chains after implantation of $_{16}O^{3+}$, $_{40}Ar^{8+}$ (figure 1 a,b) and $_{84}Kr^{15+}$ (figure 1 c), respectively.

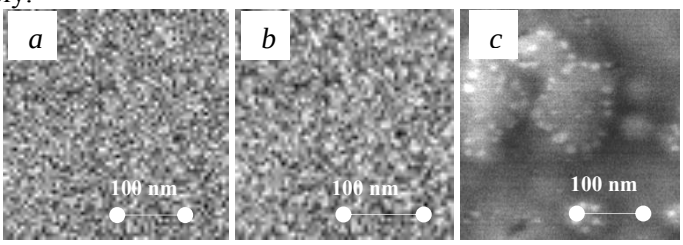

Figure 1. SEM images of the surface implanted with $_{16}O^{3+}$ (a), $_{40}Ar^{8+}$ (b) and $_{84}Kr^{15+}$ (c) ions.

The comparison of the results shows that formation of tracks on the Ni-Ti alloy surface requires high energy of the heavy ion (≥150 MeV). However, this is not sufficient according to previous studies with high-energy krypton ions used [5], when hemispherical convex structures (globules) with a size of up to 200 nm were observed after implantation up to the fluences of 5×10^{15} and $\geq5\times10^{19}$ion/m^2. The probability of track formation depends not only on the number of incident ions, but, apparently, on the ratio of B19'/B2 phases of titanium nickelide. Note that in this research we

studied the samples of the two-phase Ni-Ti alloy with higher (~ 0.7) ratio of these phases than that of the samples studied previously.

In figure 2 the data of X-ray diffraction analysis obtained for a divergent beam mode shows that the phase composition nearby the out-range area (the depth of the analysis is comparable with the calculated ion range), as well as the structure of the implanted surface depend on the ion mass. In the case of $_{16}O^{3+}$ ion implantation (figure 2, curve 2), partial radiation-stimulated phase transformation B19'→B2 can be observed. The martensite content ~3.5 times decreases compared to unimplanted Ni-Ti alloy (figure 2, curve 1). However, $_{40}Ar^{8+}$ ion implantation (figure 2, curve 3) and $_{84}Kr^{15+}$ ion implantation (figure 2, curve 4) are characterized by complete radiation-stimulated phase transformation B19'→B2 followed by dissolving Ti phase and Ni_3Ti_3O compound. As a result of this implantation, Ni-Ti alloy becomes single phase with the B2 structure (austenite).

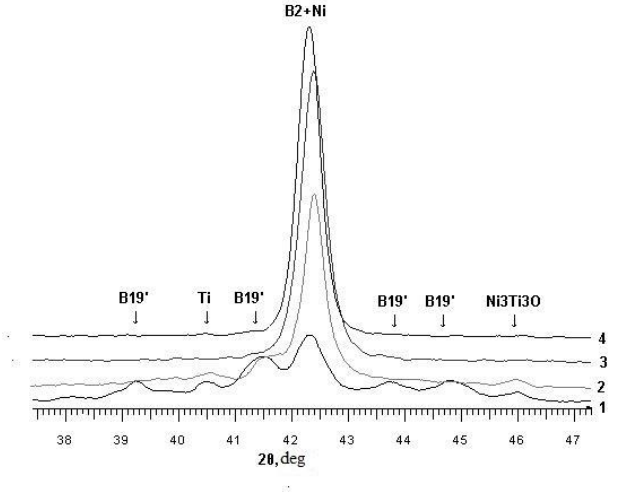

Figure 2. Parts of diffraction patterns for Ni-Ti alloy before (curve 1) and after $_{16}O^{3+}$ ion implantation (curve 2), $_{40}Ar^{8+}$ ion implantation (curve 3) and $_{84}Kr^{15+}$ ion implantation (curve 4).

Note that as the ion mass increases, the intensity of the primary X-ray line (110) of the B2 structure grows. The parameter of the body-centered cubic structure compared to unimplanted Ni-Ti alloy reduces, and this indicates approaching to the stoichiometric composition of titanium nickelide.

Similar patterns of change in the phase composition of the surface layer after $_{16}O^{3+}$, $_{40}Ar^{8+}$ and $_{84}Kr^{15+}$ ion implantation were obtained by shooting in grazing (2°) beam (analysis depth ~ 1 μm). In addition, firstly, in contrast to the out-range area, we detected slight splitting of the X-ray reflection line (110) of the B2 structure. This, as reported in [5,9,10], confirms the formation of nanoparticles of the R-phase during $_{16}O^{3+}$ ion implantation.

Secondly, the content of Ni_3Ti_3O compound does not virtually change in the out-range area and considerably reduces in the surface layer. This implies that the strain-hardened layer, formed on the Ni-Ti surface due to the technology used for its preparation, is partially sputtered during $_{16}O^{3+}$ ion implantation, its base being the Ni_3Ti_3O compound.

Earlier, the data obtained in SEM-studies of the Ni-Ti alloy surface etched prior to implantation [5] were used to attribute the surface layer hardening to titanium oxide formation during sample preparation. To make it more exact we conducted additional research in the geometry of the grazing beam at an angle of 1° to the etched surface of Ni-Ti alloy by X-ray structural analysis. The surface was found to get enriched with titanium due to release of nickel during chemical etching. This confirms the data obtained in X-ray analysis, especially as the technology of sample preparation was based on mechanical methods only.

Data on microhardness of Ni-Ti alloy measured after $_{16}O^{3+}$, $_{40}Ar^{8+}$ and $_{84}Kr^{15+}$ ion implantation indicates that, in contrast to the unimplanted alloy, distinct indentation appears even under very low (0.098 N) load. This is another evidence for the sputtering of the strain-hardened layer in interaction of heavy ions with the polished surface.

The data obtained in microhardness measurement indicates that the double-layer structure of the near-surface layer is formed with different degrees of hardening regardless of the ion mass. Radiation

hardening of the second layer with a thickness of about 1.1–1.2 μm is 71, 50 and 39% for $_{16}O^{3+}$, $_{40}Ar^{8+}$ and $_{84}Kr^{15+}$ ions, respectively. Radiation hardening in the out-range area is significantly lower (7.2, 8.9 and 16%) and, vice versa, as the weight of the heavy ion grows, it increases.

The data for the temperature dependence of the resistivity of Ni-Ti alloy after $_{16}O^{3+}$, $_{40}Ar^{8+}$ и $_{84}Kr^{15+}$ ion implantation is shown in figure 3. In comparison to the corresponding R (T)-curves, measured before implantation, the martensitic transformation (MT) temperature range shifts and widens, the shape and area of the electrical resistance hysteresis loop changes. All the loops are straight, and the degree of variation depends on the ion mass, as in the case of the structure.

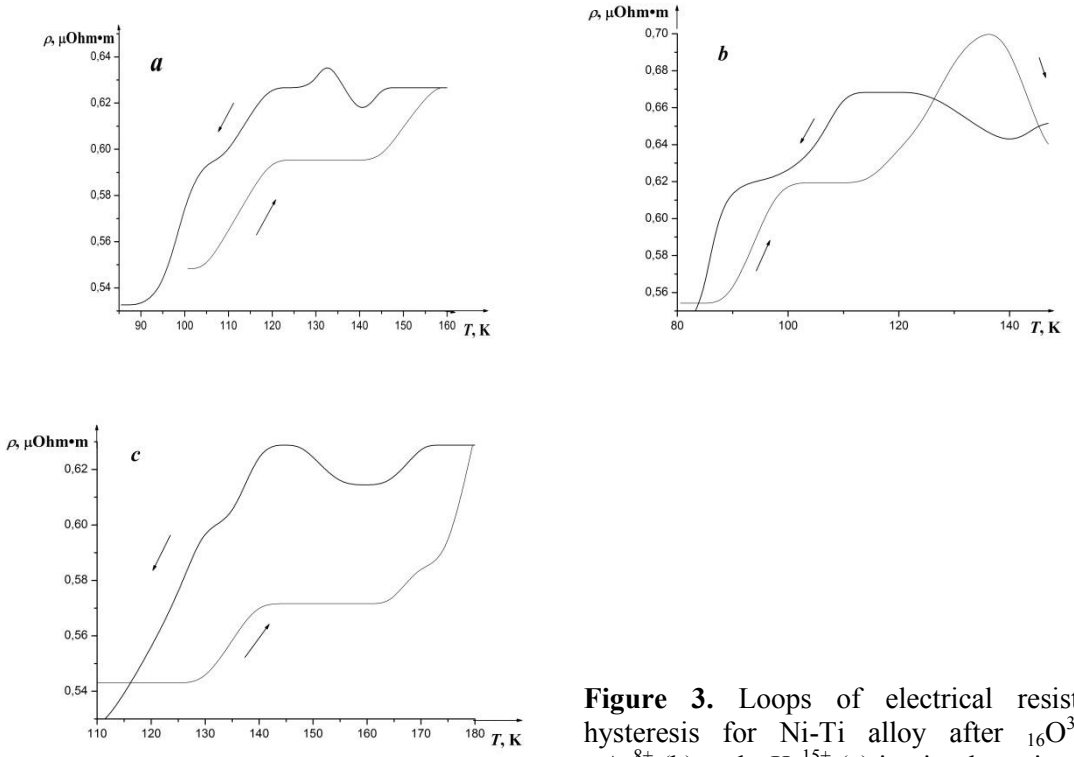

Figure 3. Loops of electrical resistivity hysteresis for Ni-Ti alloy after $_{16}O^{3+}$ (a), $_{40}Ar^{8+}$ (b) and $_{84}Kr^{15+}$ (c) ion implantation.

It was found that under the impact of $_{16}O^{3+}$ ions the temperature range shifts towards lower MT temperatures and 3.6 times increases mainly due to the greater degree of decrease in the temperature of M_{end} (figure 3 a). Martensitic transformation is preceded by pre-martensitic phase transformation B2→R, which indicates positive values of dρ/dT coefficients [11]. Changing of the shape and area of the electrical resistance hysteresis loop is related to the pre-martensitic transformation and extending temperature range reverse to MT due to a significant increase in temperature when it ends A_{end}.

As the mass of inert gases increases, the MT temperature range shifts, on the contrary, towards higher temperatures, and its widening is due to the greater degree of the increase in the temperature when MT starts M_{st}. In the case of $_{40}Ar^{8+}$ ion implantation (figure 3 b), firstly, direct MT is of distinctly stepped character compared to $_{16}O^{3+}$ ion implantation (figure 3 a) and $_{84}Kr^{15+}$ ion implantation (figure 3 c).

Secondly, in the R(T)-curve of the inverse martensite transformation we can find the electric resistance scale maximum exceeding by 0.033 μOhm·m compared to the temperature of the start M_{st} of the direct MP, and then a sharp decline as the temperature keeps increasing. A similar effect has been previously observed after heat treatment of nickel-titanium alloys doped with the third component [12].

Note that for both ions of inert gases the pre-martensitic transformation area is more extended and more pronounced. It contains the region where electrical resistance increases as the temperature falls, and the "plateau" with ρ = const in the R-curve of direct MT (figure 3 b and c). According to [12], two processes are responsible for this "plateau". The first one is related to crystal lattice distortions in

transition of the R-phase, which increases electrical resistance, and the second one caused by the decrease in the amplitude of thermal vibrations (phonon component of the electric resistance) contributes to electrical resistance reduction.

The process of phase transformation B2→R in heavy ion implantation to a relatively low fluence determined by measuring the temperature dependence of the resistivity is consistent with its greater sensitivity as compared to the results of X-ray analysis.

4. Conclusion

In the experimental study, we found the features of the impact of implantation of Ni-Ti alloy with $_{16}O^{3+}$, $_{40}Ar^{8+}$ and $_{84}Kr^{15+}$ heavy ions on its structure, phase composition, and physical and mechanical properties under relatively similar parameters A/Z, E_{ion}/a.e.m., Φ and J_{beam}. The direct relationship between increase in the ion mass and radiation damage of Ni-Ti alloy with the shape memory effect is not found, but it is manifested in the degree of the processes, namely, sputtering, track formation, phase transformations and changes in the temperature ranges of martensitic transformations.

The preliminary testing of Ni-Ti alloy revealed the following features of radiation damage when exposed to $_{16}O^{3+}$, $_{40}Ar^{8+}$ and $_{84}Kr^{15+}$ ions:

- the process of sputtering prevails in the case of lighter $_{16}O^{3+}$ ions, and the process of ion etching dominates under the effect of $_{84}Kr^{15+}$ heavy ions. The strain-hardened layer based on Ni_3Ti_3O compound is dispersed regardless of the ion mass;
- for ions with M≤40, the formation of ~ 1 nm-sized bubbles can be observed, whereas, in the case of $_{84}Kr^{15+}$ ions, we observe tracks with a dome surrounded by bubble chains;
- in implantation, partial ($_{16}O^{3+}$) and complete (M≥40) radiation-induced phase transformation B19'→B2 occurs both in the near-surface layer and nearby the out-range area. The phase composition of titanium nikelid consists mainly of the B2 structure (austenite);
- regardless of the ion mass, the near-surface layer is a double layer structure. As the mass of the ion increases, the degree of the second layer hardening decreases from 71 to 39%. In the out-range area, on the contrary, it grows from 7 to 16%;
- the martensitic transformation temperature range with pre-martensitic phase transformation B2→R is found to shift towards lower and higher temperatures for $_{16}O^{3+}$ ions and M≥40, respectively.

The results obtained suggest new possibilities for modification by different heavy ions of gaseous elements to make titanium nickelid alloys for medical use which are radiation-resistant to ionizing radiation and retain the ability of the shape memory effect.

Acknowledgements

This work was partially supported by The Ministry of Education and Science of the Russian Federation within the framework of the government “Science” program.

References

[1] Kislitsin S B, Poltavtseva V P and Antoniuc V I 2009 *Proc. 8 Int. Conf. on the Interaction of Radiation with Solids* (Minsk: Publishing House Center BSU) pp 92-94
[2] Poltavtseva V P 2010 *Proc. of the 10th Int. Conf. on Modification of materials with particle beams and plasma flows* (Tomsk: Publishing House) pp 441–442
[3] Poltavtseva V P, Antoniuc V I and Kireev V V 2011 *Proc. VIII Int. Conf. in Fundamental and Applied Materials Science* (Barnaul: Publishing House AltSTU) pp 65–69
[4] Poltavtseva V P, Kislitsin S B, Koval N N and Oskomov K V 2012 *Izv. Vyssh. Uchebn. Zaved. Fiz.* **12/3** 41–43
[5] Poltavtseva V P, Kislitsin S B, Koval N N and Antoniuc V I 2013 *Proc. 10 Int. Conf. on Interaction of Radiation with Solids* (Minsk: Publishing House of BSU Center) pp 211–213
[6] Poltavtseva V P, Kislitsin S B and Antoniuc V I 2014 *Abstracts of Int. Congress on Energy Fluxes and Radiation Effects* (Tomsk: Publishing House of IAO SB RAS) p 265
[7] Poltavtseva V P, Kislitsin S B, Antoniuc V I and Satpaev D A 2013 *Proc. 9 Int. Conf. on*

Nuclear and Radiation Physics (Almaty: RSE INP) pp 103–104
[8] Poltavtseva V P, Kislitsin S B and Antoniuc V I 2009 *Izv. Vyssh. Uchebn. Zaved. Fiz.* **12/3** pp 41–43.
[9] G.E. Gunther, V.N. Khodorenko, Y.F. Yasenchuk et al. 2006 *Titanium Nikelide. Medicalapplience of New Generation* (Tomsk: MEC)
[10] Lotkov A I, Grishkov V N, Anokhin S V and Kuznetsov A I 1982 *Izv. Vyssh. Uchebn. Zaved. Fiz.* **10** pp 11–16.
[11] Potekaev A I, Klopotov A A, Kozlov E V and Kulagin V V 2004 *Weak-stable Pretransitional Structures in Ttitanium Nickelide* (Tomsk: STL)
[12] Honma Toshio and Takei Hiromi 1975 *Nippon Kinzoku Gakkaishi/Journal of the Japan Institute of Metals* **39(2)** pp 175–182